Available online at www.sciencedirect.com
ScienceDirect
Journal of Environmental Sciences 2011, 23(1) 51–59
JOURNAL OF ENVIRONMENTAL SCIENCES
ISSN 1001-0742
CN 11-2629/X
www.jesc.ac.cn

Potential particulate pollution derived from UV-induced degradation of odorous dimethyl sulfide

Liping Qiao, Jianmin Chen*, Xin Yang*

Center for Atmospheric Chemistry Studies, Department of Environmental Science & Engineering, Fudan University, Shanghai 200433, China. E-mail: 071047002@fudan.edu.cn

Received 28 June 2010; revised 27 August 2010; accepted 31 August 2010

Abstract

UV-induced degradation of odorous dimethyl sulfide (DMS) was carried out in a static White cell chamber with UV irradiation. The combination of *in situ* Fourier transform infrared (FT-IR) spectrometer, gas chromatograph-mass spectrometer (GC-MS), wide-range particle spectrometer (WPS) technique, filter sampling and ion chromatographic (IC) analysis was used to monitor the gaseous and potential particulate products. During 240 min of UV irradiation, the degradation efficiency of DMS attained 20.9%, and partially oxidized sulfur-containing gaseous products, such as sulfur dioxide (SO_2), carbonyl sulfide (OCS), dimethyl sulfoxide (DMSO), dimethyl sulfone ($DMSO_2$) and dimethyl disulfide (DMDS) were identified by *in situ* FT-IR and GC-MS analysis, respectively. Accompanying with the oxidation of DMS, suspended particles were directly detected to be formed by WPS techniques. These particles were measured mainly in the size range of accumulation mode, and increased their count median diameter throughout the whole removal process. IC analysis of the filter samples revealed that methanesulfonic acid (MSA), sulfuric acid (H_2SO_4) and other unidentified chemicals accounted for the major non-refractory compositions of these particles. Based on products analysis and possible intermediates formed, the degradation pathways of DMS were proposed as the combination of the $O(^1D)$- and the OH- initiated oxidation mechanisms. A plausible formation mechanism of the suspended particles was also analyzed. It is concluded that UV-induced degradation of odorous DMS is potentially a source of particulate pollutants in the atmosphere.

Key words: UV irradiation; photodegradation; dimethyl sulfide; particulate pollutants; odorous emission

DOI: 10.1016/S1001-0742(10)60372-5

Citation: Qiao L P, Chen J M, Yang X, 2011. Potential particulate pollution derived from UV-induced degradation of odorous dimethyl sulfide. *Journal of Environmental Sciences*, 23(1): 51–59.

Introduction

Odorous emission is commonly associated with industrial or agricultural processes such as pulp and paper manufacturing, oil or petroleum refining, composting, landfilling, slaughtering and sewage or wastewater treatment (Dincer and Muezzinoglu, 2006; Ras et al., 2008). Dimethyl sulfide (DMS) is a typical gaseous odor pollutant owing to its offensive smells with a very low odor threshold value of 0.6–40 ppb and extreme negative hedonic characteristics (Demeestere et al., 2005). At ambient levels, the odor of DMS does not necessarily pose a health hazard (Shu and Chen, 2009). However, high concentration exposure to DMS in short term can cause lung congestion, diarrhea, stomach pain and several other body ailments, and may even lead to suffocation or death (Jäppinen et al., 1993; Terazawa et al., 1991). Therefore, the removal or degradation of DMS odorant before exhausting into the atmosphere will be of great significance to improve the local air quality and to safeguard human health.

Nowadays, there are many physical-chemical and biological techniques to remove DMS in the polluted air streams before exhausting into the atmosphere. Because of the ecological and economical advantages, biological waste gas treatments such as biofilters (Liu et al., 2008; Zhang et al., 2008), biotrickling filters (Luvsanjamba et al., 2008b; Sercu et al., 2007) and membrane bioreactors (Luvsanjamba et al., 2008a) are widely used for odorous gases removal, especially for odors at low concentrations. However, DMS is one of the least biodegradable compounds among the odorous sulfur-containing gaseous pollutants; consequently, it always needs improved systems out of the conventional biological setups (De Bo et al., 2003; Sercu et al., 2005). And the elevated temperatures (45–75°C) in some DMS emission processes such as pulp and paper manufacturing and composting can directly decrease the removal efficiency of odors (Luvsanjamba et al., 2008b). Moreover, the long-term performance of the biological systems is easily reduced due to many physical and chemical parameters including acidification, pressure drops, fouling, accumulation of inhibiting salts, and drying

* Corresponding author. E-mail: jmchen@fudan.edu.cn (Jianmin Chen); yangxin@fudan.edu.cn (Xin Yang).

of the filter bed (De Bo et al., 2003; Jarrige and Vervisch, 2007).

Traditional physical-chemical approaches to DMS removal mainly include wet scrubbing, adsorption and chemisorption (Goyal et al., 2008; Tanada et al., 1978). These approaches mainly transform the pollutants from gas phase to solid or liquid phase; consequently, always require large amounts of chemicals and following secondary wastes disposal which imply a high cost. In recent years, some novel physical-chemical methods are emerging or employed for deodorization. Due to the known advantages such as high removal efficiency at relatively low reaction temperatures and complete mineralization properties, these methods that involve photodissociation (Barr et al., 2004; Martinez-Haya et al., 1999), electron-beam irradiation (Hakoda et al., 2009), corona discharge decomposition (Chen et al., 2009; Jarrige and Vervisch, 2007; Yang et al., 2009), catalytic (Devulapelli and Sahle-Demessie, 2008; Gonzalez-Garcia et al., 2004; Sahle-Demessie and Devulapelli, 2008) and ozone oxidation (Du et al., 2007; Wang et al., 2007) become attractive and promising. Nevertheless, among these methods, photodissociation, electron-beam irradiation and corona discharge decomposition commonly imply high energy consumption especially for much diluted emissions. Catalytic and ozone catalytic oxidation always encounter sulfur-poisoning effects on catalysts and are typically adopted to lower the concentrations of inlet gases. Another important barrier to the extensive application of these emerging approaches is the nondestructive potentials and the probably poisonous intermediates.

Until now, the drawbacks of these physical-chemical and biological techniques are focused either on the DMS removal efficiency and the corresponding operational parameters that affect conversion or on the financial cost that comes from chemicals and energy consumption (Devulapelli and Sahle-Demessie, 2008; Jarrige and Vervisch, 2007; Zhang et al., 2007, 2008). Limited publications have reported the potential toxicity from the reaction intermediates. However, current literature is still blank to discuss the environmental benignancy of the end products of odorous DMS degradation.

The objective of this study was focused on the end products of the photooxidation removal of DMS. The potential particulate pollution in this process was also revealed.

1 Experimental

1.1 Experimental setup and procedures

The UV-induced degradation setup employed in the experiments was a 14 L borosilicate glass reaction chamber (Cell 45-V, Infrared Analysis Inc., USA) equipped with tubular quartz filtered low-pressure mercury lamp (15 W, λ_{max} = 254 nm, Jelight Co., USA) (Fig. 1). On the top of the chamber, one inlet with silicone gasket was for reactants injection or for sample taking by solid-phase micro-extraction (SPME) method, and the other with

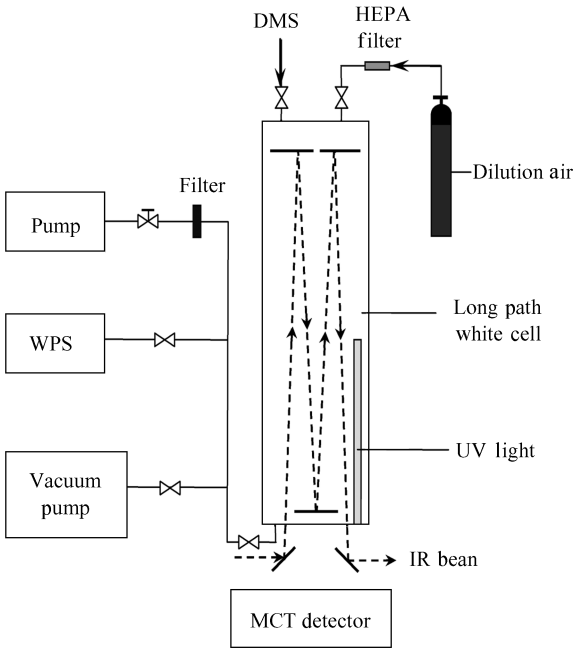

Fig. 1 Schematic diagram of the apparatus. DMS: dimethyl sulfide; WPS: wide-range particle spectrometer; MCT: mercury-cadmium-telluride.

HEPA-filter was for the introduction of the dilution gas, i.e., high-purity air with 20.0 ppm of H_2O. On the bottom of the chamber, an outlet was set either for vacuumizing if connected with vacuum pump or for sampling if connected with analysis instruments.

DMS photodegradation experiments were conducted at ambient pressure and at (25 ± 2)°C in a static mode (i.e., batch reactor). For each experiment, a certain amount of DMS was injected into the reactor and evaporated for 20 min in the vacuum below 100 Pa, and then the dilution air was introduced until meeting the ambient pressure. After 30 min of mixing, turned on the UV light and the reaction was initiated. Typically, the initial concentration of DMS was controlled at 23.0 ppm for each experiment.

1.2 Gaseous products monitoring

The reactant of odorous DMS and gaseous products were monitored *in situ* using a multi-reflection White mirror system (31.1 m optical path length) mounted in the chamber and coupled to a Fourier transform infrared (FT-IR) spectrometer (Nicolet Avatar 380, Thermo Electron corp., USA) equipped with mercury-cadmium-telluride (MCT) detector. Generally, IR spectra were recorded in the spectral range from 4000 to 650 cm^{-1} at a resolution of 4 cm^{-1}, and 64 scans were averaged for each spectrum result in a time resolution of 1 min. The identification of the reactant and products was mainly achieved by computer-aided subtraction of calibrated reference spectra.

The reactant and major partial oxidation products were also identified by analyzing them with an Agilent 6890 Series gas chromatograph-mass spectrometer (GC-MS) equipped with an HP-5MS (30 m × 0.32 mm × 0.25 μm) column. The gas samples were extracted using a carboxen/polydimethylsiloxane SPME fiber (75 μm,

Sigma-Aldrich Co., USA) assembled on 57330-U SPME holder (Supelco, USA) and injected immediately into the GC-MS injection port.

1.3 Measurement of suspended particles

Suspended particles were directly detected using a wide-range particle spectrometer (WPS, Model 1000XP, MSP Co., USA) covering the diameter range of 10–10000 nm. The size distribution of the particles was also recorded. The WPS was operated at wide-range mode with 84 particle-size channels and the channel scanning was controlled to accomplish in 120 sec. The flow rate was kept constant at 1.00 L/min. While sampling, ambient air was introduced into the reactor through an activated charcoal filter and an HEPA filter to maintain the pressure equilibrium in the reactor.

Teflon filter (pore size: 0.4 μm, diameter: 47 mm), a flow controller and a mechanic pump were used to collect the suspended particles formed in the photodegradation of odorous DMS. After collection, the sample filter was extracted ultrasonically by 5.00 mL deionized water. Then the filtrations, obtained by passing through 0.45 μm microporous membranes, were analyzed by ion chromatography (IC, Dionex ICS-3000, Dionex Corp., USA). The gradient weak base eluent (76.2 mmol/L NaOH + H_2O) was used for anion detection.

2 Results and discussion

2.1 Degradation efficiency and gaseous products

Figure 2 illustrates the variation of the *in situ* FT-IR spectra of the UV-induced degradation of odorous DMS. As can be seen, the absorption bands of DMS, features at 2974 and 2937 cm^{-1} (antisymmetric stretch of methyl group CH_3, $\nu^{as}_{CH_3}$), 2859 cm^{-1} (symmetric stretch of CH_3, $\nu^{s}_{CH_3}$), 1436 cm^{-1} (antisymmetric deformation of CH_3, $\delta^{as}_{CH_3}$), 1311 cm^{-1} (symmetric deformation of CH_3, $\delta^{s}_{CH_3}$), 1016 and 974 cm^{-1} (rock of CH_3, ρ_{CH_3}), decreased drastically in intensity as the photochemical reaction proceeded, which implied the degradation of odorous DMS. Further analysis revealed a degradation efficiency of 20.9% during 240 min of UV irradiation, corresponding to the concentration of DMS reduced from 23.0 to 18.2 ppm. The residual concentration of DMS ([DMS], ppm) exhibited excellent linear relationship with the irradiation time (t, min) as follows:

$$[\mathrm{DMS}] = 22.9 - 0.021 \times t \qquad R^2 = 0.996 \qquad (1)$$

Except for the decrease of the feature bands of DMS, some new absorption bands appeared in the FT-IR spectra with reaction undergoing. The bands at 1372 and 1350 cm^{-1} ($\nu^{as}_{S=O}$), 1166 cm^{-1} ($\nu^{s}_{S=O}$), 2510 and 2487 cm^{-1} (overtone bands of $\nu^{as}_{S=O}$) attributed to gaseous sulfur dioxide (SO_2), at 2804 cm^{-1} (ν^{as}_{C-H}), 2756 cm^{-1} (ν^{s}_{C-H}), 1769, 1754 and 1721 cm^{-1} ($\nu^{as}_{(H-)C=O}$) corresponding to formaldehyde (HCHO), at 1791 cm^{-1} ($\nu^{as}_{(O-)C=O}$) characterizing of formic acid (HCOOH), and at 2362 cm^{-1} ($\nu^{as}_{C=O}$, P branch) and 2334 cm^{-1} ($\nu^{as}_{C=O}$, Q branch) featuring for gaseous carbon dioxide (CO_2) all continuously grew in intensity as the absorption bands of gaseous DMS decreased. In addition, several weak absorption bands with peaks at 2173, 2116, 2073, 2050, 1123, 1094 and 818 cm^{-1} appeared in the spectra and increased in intensity with reaction time. The bands centered at 2173 cm^{-1} ($\nu^{as}_{C\equiv O}$, P branch) and 2116 cm^{-1} ($\nu^{as}_{C\equiv O}$, Q branch) are attributed to gaseous carbon monoxide (CO). The gaseous carbonyl sulfide (OCS) with bands at 2073 and 2050 cm^{-1} is proposed to be the intermediate species of DMS oxidation according to previous studies (Barnes et al., 1994). The appearance of the bands at 1123 cm^{-1} ($\nu^{s}_{(O=)S=O}$), 1094 cm^{-1} ($\nu^{s}_{S=O}$) and 818 cm^{-1} ($\nu^{as}_{(C-)S-O}$) is characteristic of the formation of intermediate species, corresponding to dimethyl sulfone ($DMSO_2$), dimethyl sulfoxide (DMSO) and methanesulfonic acid (MSA), respectively.

Figure 3 presents a GC-MS chromatogram and typical mass patterns for the intermediates after 240 min of reaction. The reactant DMS was detected at 1.00 min in the GC-MS chromatogram. And SO_2, dimethyl disulfide (DMDS), DMSO and $DMSO_2$ which were identified as gas phase reaction products were detected at 0.85, 1.56, 2.67 and 3.66 min, respectively, in GC-MS chromatogram. Such results were consistent with the FT-IR analysis except DMDS.

2.2 Detection of suspended particles and size distribution characteristics

In addition to the *in situ* FT-IR monitoring, WPS was applied to detect the end products probably existing in solid or liquid phase (i.e., aerosol particles). Figure 4 shows a typical time-series count size distribution of particles formed in the degradation process. Firstly, the results of control experiments (Fig. 4), i.e., experiments in a cleaned chamber to UV light or in a non-illuminated chamber containing high-purity air diluted DMS, indicated that particles can be formed neither under the dark conditions nor under the blank conditions. Secondly, the results of the UV-irradiated experiment with DMS diluted by high-purity nitrogen verified that the particles cannot be produced without oxygen and other oxidants.

In the DMS degradation experiments, the time that UV light was turned on was recorded as time zero. After 15 min, a strong count concentration peak was detected at 68–73 nm, indicating a rapid and substantial formation of suspended particles. With irradiation time extending, the count concentration peak shifted to larger size and reached 425 nm after 240 min, which was consistent with the condensation growth cases. The particles below 10 nm were excluded in this study because of the stated minimum measurable size (10 nm) of WPS. In the experiments, 68–73 nm at 15 min was identified as the initial peak diameter, which implied that the particles might grow or condense rapidly once the initial nucleation occurred and small suspended particles at nuclei mode were formed.

Lognormal function, which often provided a good fit and was regularly used in atmospheric aerosol applications (Seinfeld and Pandis, 2006), was applied to further analyze the size distribution data obtained by WPS techniques. The

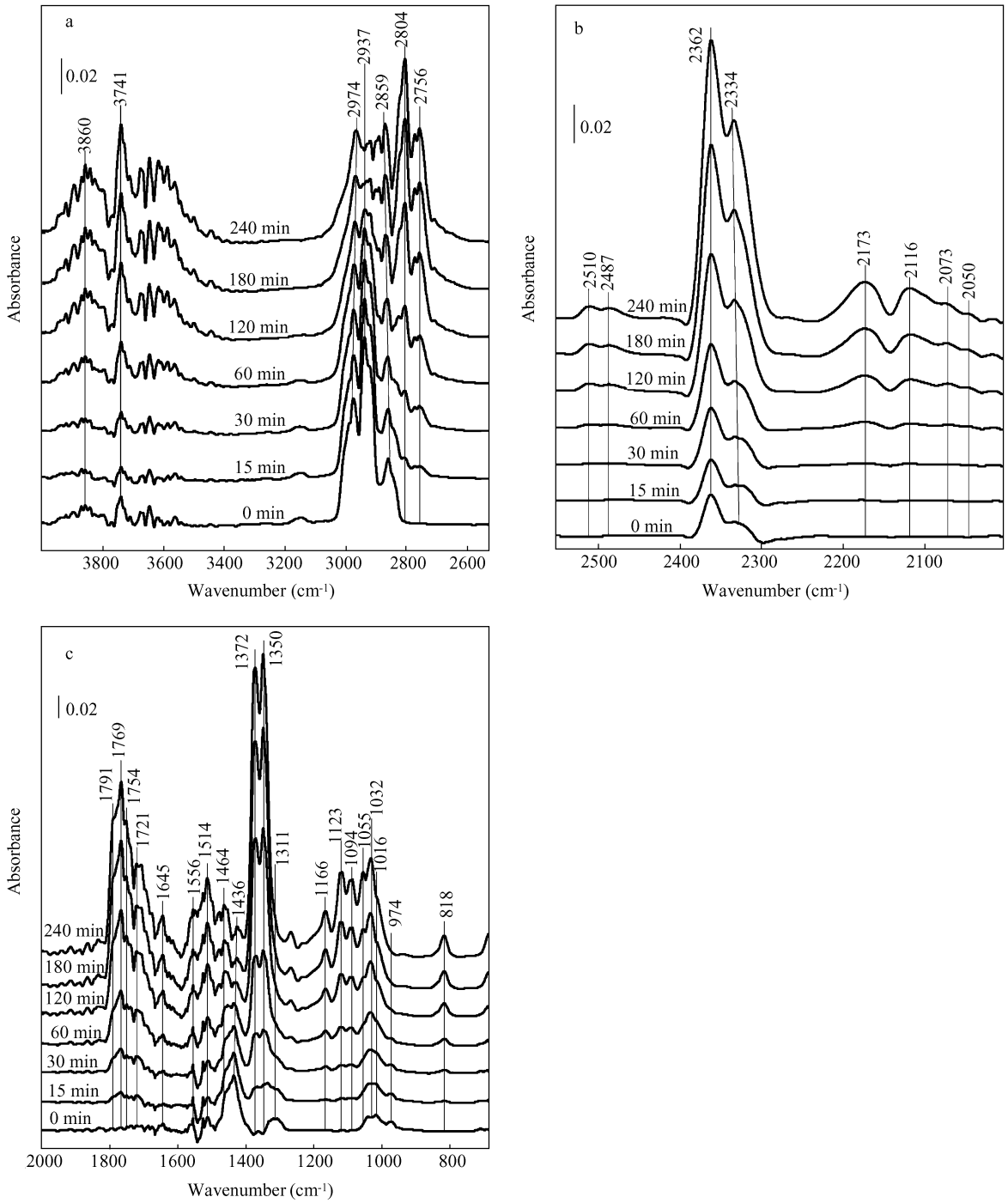

Fig. 2 *In situ* FT-IR spectra of the UV-induced degradation of odorous DMS in the wavenumbers of 4000–2530 cm^{-1} (a), 2600–2000 cm^{-1} (b), and 2000–680 cm^{-1} (c).

lognormal fitting parameters of the count size distributions for fresh aerosol particles derived from the UV-induced degradation of DMS are summarized in Table 1. As can be seen, the lognormal fitting curves fitted well with the real count size distributions of the suspended particles. The suspended particles formed after the initial 15 min of irradiation showed an excellent unimodal lognormal distribution (R^2 = 0.999) with count median diameter (CMD) at 74 nm. With reaction undergoing, the count size distribution of the fresh aerosol particles moved towards multimode. Typically, the measured count size distribution at 60 min could be well represented by two overlapping lognormal distributions (also called a bimodal distribution) with high correlation (R^2 = 0.997), which located the CMD at 76 and 91 nm, respectively. And the count size distribution at 240 min could be matched by five overlapping lognormal distributions (R^2 = 0.930) with the CMD at 13, 85, 228, 309 and 440 nm, respectively. It is noted that the suspended particles observed mainly concentrated in the accumulation mode which covered the size range of 50–2000 nm in diameter. Although particles located in Aitken mode were also observed in the 120–240 min

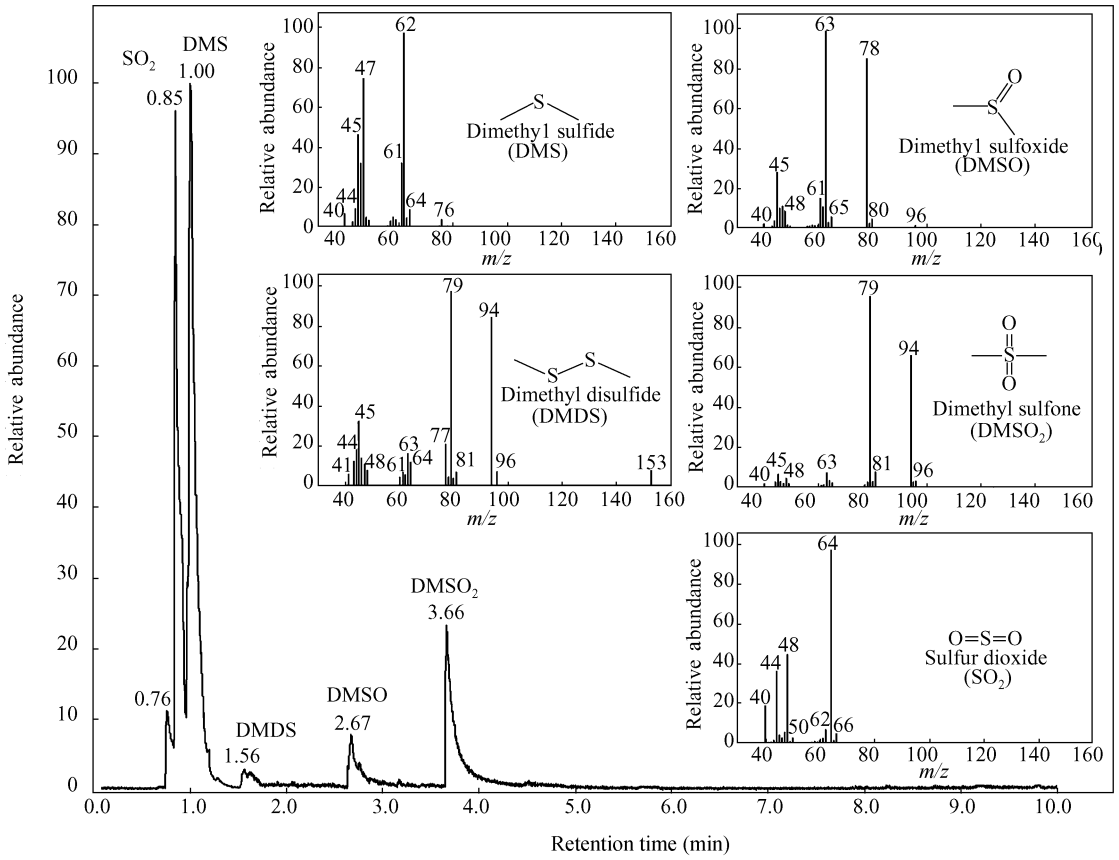

Fig. 3 GC-MS chromatogram and mass patterns for the intermediates after 240 min of reaction.

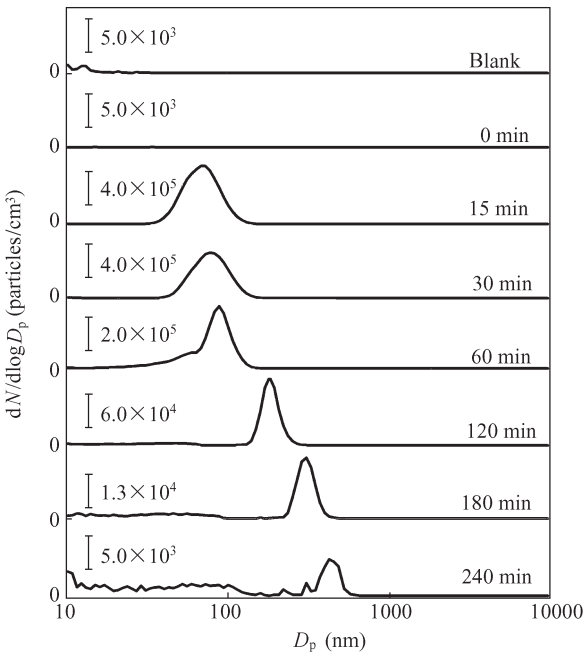

Fig. 4 Time-series count size distribution of suspended particles (D_P) detected accompanying with the degradation of odorous DMS under UV irradiation.

cases, their concentration was much lower than that in the accumulation mode. The data also showed that CMD kept increasing throughout the whole removal process, while the total number concentration of particles decayed with photoreaction undergoing. The different variation trends of the CMD and number concentration revealed two possible mechanisms with regard to the formation of the suspended particles. Firstly, the continuous increase of the median diameter was consistent with the condensational growth of particles (Kulmala and Kerminen, 2008). Secondly, the decrease of number concentration indicated that agglomeration and wall loss might take place in the whole process.

2.3 Non-refractory compositions of the suspended particles

As shown in Fig. 5, several anion peaks were detected in the sample collected on the filter. Qualitative analysis attributed the strong peaks typically at 8.98 and 27.79 min to $CH_3SO_3^-$ and SO_4^{2-} anions which were potentially resolved from MSA and H_2SO_4, respectively. Also several weak anion peaks were noticed in Fig. 5, but they were difficult to be quantified and assigned. The results were consistent with the conclusions deduced by Arsene et al. (1999) in exploring the OH-initiated photochemistry of marine DMS, that anions of SO_4^{2-}, $CH_3SO_3^-$ and $CH_3SO_2^-$ were detected in the condensate samples collected by using an ethanol-liquid nitrogen slush bath with low temperature (–157°C). The IC analysis provided evidence in addition to the WPS results that suspended particles were formed in the photodegradation of odorous DMS. And MSA, H_2SO_4 and other unidentified chemicals accounted for the major non-refractory compositions of those suspended particles.

Table 1 Lognormal fitting parameters of count size distributions for fresh suspended particles derived from the UV-induced degradation of DMS*

Time (min)	Mode I			Mode II			Mode III		
	N_1 (cm^{-3})	$\overline{D}_{p1}$ (nm)	δ_1	N_2 (cm^{-3})	$\overline{D}_{p2}$ (nm)	δ_2	N_3 (cm^{-3})	$\overline{D}_{p3}$ (nm)	δ_3
15	1.85×10^5	74	1.292						
30	1.45×10^5	83	1.291						
60	4.84×10^4	91	1.151	3.45×10^4	76	1.519			
120	1.53×10^4	185	1.126	1837	49	2.042			
180	3249	308	1.133	833	58	1.540	758	16	1.664
240	701	440	1.125	62	309	1.033	691	228	1.011

Time (min)	Mode IV			Mode V			N_t** (cm^{-3})	R^2
	N_4 (cm^{-3})	$\overline{D}_{p4}$ (nm)	δ_4	N_5 (cm^{-3})	$\overline{D}_{p5}$ (nm)	δ_5		
15							1.85×10^5	0.999
30							1.45×10^5	0.999
60							8.29×10^4	0.997
120							1.71×10^4	0.997
180							4840	0.998
240	649	85	1.568	2547	13	3.681	4650	0.930

* Parameters were derived from the lognormal function, i.e., $n_N^o(\log D_p) = \frac{dN}{d\log D_p} = \sum_{i=1}^{n} \frac{N_i}{(2\pi)^{1/2}\log\sigma_i} \exp\left(-\frac{(\log D_p - \log \overline{D}_{pi})^2}{2\log^2 \sigma_i}\right)$, where D_p is the particle size, $n_N^o(\log D_p)$ represents the number distribution with respect to $\log D_p$, N_i is the number concentration (i = 1, 2, 3, ...), $\overline{D}_{pi}$ is the count median diameter (CMD), and δ_i is the standard deviation of the ith lognormal mode.

** N_t represents the total number concentration of particles in each mode, therefore $N_t = \sum_{i=1}^{n} N_i$.

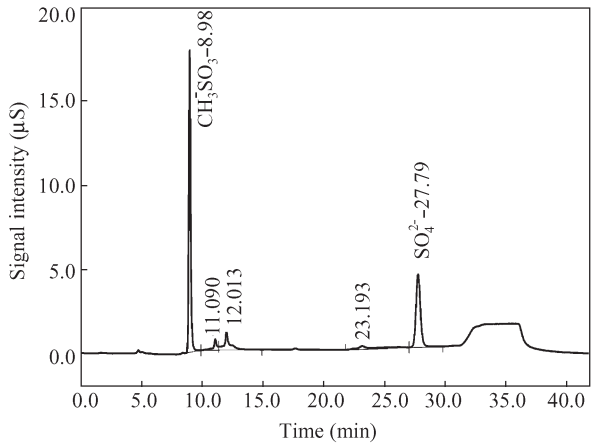

Fig. 5 Example of chromatogram demonstrating the detection and resolution of IC measurement of $CH_3SO_3^-$ and SO_4^{2-} in samples collected the suspended particles.

2.4 Proposed degradation pathways

As *in situ* FT-IR and GC-MS identification shown, SO_2, OCS, DMSO, $DMSO_2$ and DMDS accounted for the major sulfur-containing gaseous intermediates in DMS removal process, and HCHO, HCOOH, CO_2, CO and H_2O were also detected as the gas phase products. The results of IC analysis revealed MSA and H_2SO_4 as reaction products existed in the suspended particles. Based on reaction products and literature data, the degradation pathways for odorous DMS degradation with UV irradiation were proposed.

In the 254 nm UV-light irradiated air/DMS mixture systems, several routines (Reactions (2)–(5)) would generate oxidizing species including O_3, $O(^1D)$ and OH. Ozone, identified by FT-IR with feature peaks at 1055 and 1032 cm^{-1}, was created through the combination of O_2 with ground state O atoms ($O(^3P)$) that was produced by the photodissociation of oxygen molecules after absorbing ultraviolet photons. Then, O_3 would be rapidly photolyzed at 254 nm and generated $O(^1D)$. And a fraction of the $O(^1D)$ atoms would react with H_2O molecules in air to generate OH radicals.

$$O_2 + h\nu \longrightarrow O(^3P) + O(^3P) \quad (2)$$

$$O(^3P) + O_2 + M(N_2, \text{wall, etc.}) \longrightarrow O_3 + M \quad (3)$$

$$O_3 + h\nu \longrightarrow O_2 + O(^1D) \quad (4)$$

$$O(^1D) + H_2O \longrightarrow OH + OH \quad (5)$$

Previous literatures reported the rate coefficients (k_{298}) to be 6.3×10^{-12}, 50×10^{-12} and 1×10^{-30} cm^3/(molecule·sec) for reactions of OH radicals, $O(^1D)$ atoms and O_3 with DMS in the atmosphere, respectively (Warneck, 2000). Obviously, $O(^1D)$ atoms were among the most reactive species for oxidizing DMS. Thus, some fractions of $O(^1D)$ would undoubtedly react with DMS. Figure 6a illustrates two potential reaction pathways of the $O(^1D)$-initiated oxidation of DMS. The $O(^1D)$ addition mechanisms would directly produce DMSO and $DMSO_2$, which on further oxidation would generate gaseous MSA and release CH_3 radicals (Sahle-Demessie and Devulapelli, 2008). Meanwhile, the $O(^1D)$ attack could also lead to the C–S bond cleavage with CH_3SO and CH_3 radicals being released. The further cleavage of C–S bond in CH_3SO would result in the formation of SO_2 which was an important precursor of gaseous H_2SO_4. The CH_3 released would be oxidized by O_2 to form HCHO which might either be further oxidized by $O(^1D)$ to form HCOOH and then be mineralized or be split under UV irradiation with CO being produced.

The proposed $O(^1D)$-initiated mechanisms confirmed

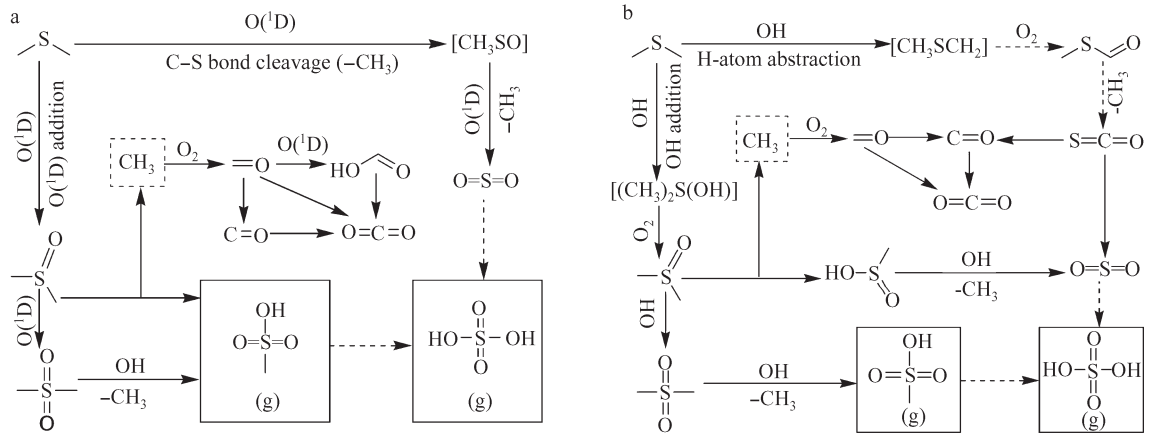

Fig. 6 Proposed degradation pathways of DMS in the present systems. (a) O(^{1}D)-initiated oxidation mechanism; (b) OH-initiated oxidation mechanism.

mostly with the FT-IR and IC products analysis. However, the FT-IR analyzed intermediates OCS cannot be explained well. Thus, the OH-initiated oxidation pathways were proposed to occur in the experimental systems, although its reactivity with DMS was little lower than that of O(^{1}D). The atmospheric chemistry of OH-initiated oxidation of DMS under different conditions has been reported detailed previously (Barnes et al., 1994, 1996). Figure 6b sketches the reactions probably took place in the present experimental systems. The OH radicals in the systems were mainly generated through Reaction (5). The reaction of OH radicals with DMS could proceed by the addition of OH to the S-atom as well as by the abstraction of a H-atom. The OH addition mechanisms would not only result in the formation of DMSO, $DMSO_2$, MSA and the release of CH_3, but might also lead to the production of methane sulfinic acid which was a precursor of SO_2. And the H-atom abstraction mechanisms were thought to generate methyl thiolformate which was expected the source of OCS in many atmospheric chemistry studies of DMS. In addition, photolysis of OCS provided another pathway for the generation of CO in the system.

The proposed O(^{1}D)- and OH- initiated mechanisms explained all products except DMDS. A possible pathway lead to DMDS might derive from the combination of CH_3S radicals which were released from the direct splitting of C–S bond in DMS molecules under the UV irradiation of 254 nm. On the whole, the degradation pathways of DMS which combined the O(^{1}D)- and OH- initiated oxidation mechanisms, although explained well the intermediates and products in the UV-induced degradation of odorous DMS, still need to be further studied.

2.5 Remarks about the formation of suspended particles

Particle formation is tied strongly with chemical processes, particularly the formation of low-volatile vapors such as sulfuric acid and multifunctional organic compounds vapors (Kulmala and Kerminen, 2008). Based on the previous analyses, once gaseous MSA and H_2SO_4 were formed through series of homogeneous chemical reactions, several competing processes might simultaneously take place for these molecules. In the first instance, these low-volatile vapors might condense by nucleation and thus produced stable clusters or new particles. It has been proposed and confirmed that homogeneous binary H_2O-H_2SO_4 nucleation was one of the most realistic candidates for nucleation mechanisms (Benson et al., 2008; Weber et al., 1999). Typically, the phase change between vapor and liquid occurred at around 1–2 nm in diameter. After homogeneous nucleation burst, the freshly-nucleated stable clusters would be driven to grow by taking the low-volatile vapors. Meanwhile, under Brownian self-coagulation as well as inter-particle forces such as van der Waals interactions and charge-image charge effects, coagulation might also occur between these freshly-nucleated clusters and induced the particles to grow (Kulmala and Kerminen, 2008). Accompanying with the formation and growth of particles, the vapors and freshly-formed particles might condense onto or be adsorbed by the reactor walls, and the larger particles would deposit onto the bottom of the reactor. However, the suspended particles were detected throughout the whole removal process.

3 Conclusions

This article presents preliminary results employing UV irradiation of 254 nm for the degradation of odorous DMS. It was revealed that SO_2, OCS, DMSO, $DMSO_2$ and DMDS accounted for the major sulfur-containing gaseous intermediates, and HCHO, HCOOH, CO_2, CO and H_2O were the oxidation products. An important finding is that, accompanying with the degradation of DMS, the formation of suspended particles was directly detected by WPS techniques. Additional evidence to verify the substantial formation of suspended particles came from the IC analysis of the filter samples that collected the suspended particles. Thus, it should be of great concern for potential particulate pollution that derived from the photodegradation of odorous DMS.

Further analysis revealed these suspended particles consisted mainly of MSA and H_2SO_4, and the count

size distribution concentrated in the accumulation mode. Once released to atmosphere, these suspended particles would become possible sources of particulate pollutants or aerosol pollution and thus threaten the human health. In addition, these acidic particles might become cloud condensation nuclei (CCN) and participated in the gas-to-particle conversion of atmospheric chemicals. In this sense, a careful analysis of the experimental data obtained from the laboratory simulation experiments will be important to appreciate the contribution of odorous DMS to the production of secondary aerosol. More study is needed to elucidate the detailed gas-to-particle mechanisms that form suspended particles in the odorous removal system.

Acknowledgments

This work was supported by the National Natural Science Foundation of China (No. 40533017, 40728006, 40875073, 40705045). This work was also partly supported by the 973 Program (No. 2008CB417205) from the Ministry of Science and Technology of China. The authors wish to thank Dr. Huiqin Guo, School of Environmental & Chemical Engineering, Nanchang Hangkong University, for her valuable writing assistance.

References

Arsene C, Barnes I, Becker K H, 1999. FT-IR product study of the photo-oxidation of dimethyl sulfide: Temperature and O_2 partial pressure dependence. *Physical Chemistry Chemical Physics*, 1(24): 5463–5470.

Barnes I, Becker K H, Patroescu I, 1994. The tropospheric oxidation of dimethyl sulfide: A new source of carbonyl sulfide. *Geophysical Research Letters*, 21(22): 2389–2392.

Barnes I, Becker K H, Patroescu I, 1996. FT-IR product study of the OH initiated oxidation of dimethyl sulphide: Observation of carbonyl sulphide and dimethyl sulphoxide. *Atmospheric Environment*, 30(10-11): 1805–1814.

Barr J, Torres I, Verdasco E, Banares L, Aoiz F J, Martinez-Haya B, 2004. Photodissociation dynamics of dimethyl sulfide following excitation within the first absorption band. *Journal of Physical Chemistry A*, 108(39): 7936–7948.

Benson D R, Young L H, Kameel F R, Lee S H, 2008. Laboratory-measured nucleation rates of sulfuric acid and water binary homogeneous nucleation from the SO_2+OH reaction. *Geophysical Research Letters*, 35: L11801. DOI: 10.1029/2008GL033387.

Chen J, Su Q F, Pan H, Wei J W, Zhang X M, Shi Y, 2009. Influence of balance gas mixture on decomposition of dimethyl sulfide in a wire-cylinder pulse corona reactor. *Chemosphere*, 75(2): 261–265.

De Bo J, Heyman J, Vincke J, Verstraete W, Van Langenhove H, 2003. Dimethyl sulfide removal from synthetic waste gas using a flat poly(dimethylsiloxane)-coated composite membrane bioreactor. *Environmental Science and Technology*, 37(18): 4228–4234.

Demeestere K, Dewulf J, De Witte B, Van Langenhove H, 2005. Titanium dioxide mediated heterogeneous photocatalytic degradation of gaseous dimethyl sulfide: Parameter study and reaction pathways. *Applied Catalysis B-Environmental*, 60(1-2): 93–106.

Devulapelli V G, Sahle-Demessie E, 2008. Catalytic oxidation of dimethyl sulfide with ozone: Effects of promoter and physico-chemical properties of metal oxide catalysts. *Applied Catalysis A–General*, 348(1): 86–93.

Dincer F, Muezzinoglu A, 2006. Chemical characterization of odors due to some industrial and urban facilities in Izmir, Turkey. *Atmospheric Environment*, 40(22): 4210–4219.

Du L, Xu Y F, Ge M F, Jia L, Yao L, Wang W G, 2007. Rate constant of the gas phase reaction of dimethyl sulfide (CH_3SCH_3) with ozone. *Chemical Physics Letters*, 436(1-3): 36–40.

Gonzalez-Garcia N, Ayllon J A, Domenech X, Peral J, 2004. TiO_2 deactivation during the gas-phase photocatalytic oxidation of dimethyl sulfide. *Applied Catalysis B–Environmental*, 52(1): 69–77.

Goyal M, Dhawan R, Bhagat M, 2008. Adsorption of dimethyl sulfide vapors by activated carbons. *Colloids and Surfaces A-Physicochemical and Engineering Aspects*, 322(1-3): 164–169.

Hakoda T, Chowdhury M A Z, Shimada A, Hirota K, 2009. Oxidation of dimethyl sulfide in air using electron-beam irradiation, and enhancement of its oxidation via an MnO_2 catalyst. *Plasma Chemistry and Plasma Processing*, 29(6): 549–557.

Jäppinen P, Kangas J, Silakoski L, Savolainen H, 1993. Volatile metabolites in occupational exposure to organic sulfur-compounds. *Archives of Toxicology*, 67(2): 104–106.

Jarrige J, Vervisch P, 2007. Decomposition of gaseous sulfide compounds in air by pulsed corona discharge. *Plasma Chemistry and Plasma Processing*, 27(3): 241–255.

Kulmala M, Kerminen V M, 2008. On the formation and growth of atmospheric nanoparticles. *Atmospheric Research*, 90(2-4): 132–150.

Liu J W, Liu J X, Li L, 2008. Performance of two biofilters with neutral and low pH treating off-gases. *Journal of Environmental Sciences*, 20(12): 1409–1414.

Luvsanjamba M, Kumar A, Van Langenhove H, 2008a. Removal of dimethyl sulfide in a thermophilic membrane bioreactor. *Journal of Chemical Technology and Biotechnology*, 83(9): 1218–1225.

Luvsanjamba M, Sercu B, Van Peteghem J, Van Langenhove H, 2008b. Long-term operation of a thermophilic biotrickling filter for removal of dimethyl sulfide. *Chemical Engineering Journal*, 142(3): 248–255.

Martinez-Haya B, Zapater I, Quintana P, Menendez M, Verdasco E, Santamaria J et al., 1999. Photodissociation of dimethyl sulfide at 227.5 nm: resonance-enhanced multiphoton ionization of the methyl fragment. *Chemical Physics Letters*, 311(3-4): 159–166.

Ras M R, Marce R M, Borrull F, 2008. Solid-phase microextraction – Gas chromatography to determine volatile organic sulfur compounds in the air at sewage treatment plants. *Talanta*, 77(2): 774–778.

Sahle-Demessie E, Devulapelli V G, 2008. Vapor phase oxidation of dimethyl sulfide with ozone over V_2O_5/TiO_2 catalyst. *Applied Catalysis B–Environmental*, 84(3-4): 408–419.

Seinfeld J H, Pandis S N, 2006. Atmospheric Chemistry and Physics: From Air Pollution to Climate Change (2nd ed.). John Wiley & Sons, Inc., Hoboken, New Jersey, USA.

Sercu B, Boon N, Beken S V, Verstraete W, Van Langenhove H, 2007. Performance and microbial analysis of defined and non-defined inocula for the removal of dimethyl sulfide in a biotrickling filter. *Biotechnology and Bioengineering*, 96(4): 661–672.

Sercu B, Nunez D, Van Langenhove H, Aroca G, Verstraete

W, 2005. Operational and microbiological aspects of a bioaugmented two-stage biotrickling filter removing hydrogen sulfide and dimethyl sulfide. *Biotechnology and Bioengineering*, 90(2): 259–269.

Shu C H, Chen C K, 2009. Enhanced removal of dimethyl sulfide from a synthetic waste gas stream using a bioreactor inoculated with *Microbacterium* sp. NTUT26 and *Pseudomonas putida*. *Journal of Industrial Microbiology and Biotechnology*, 36(1): 95–104.

Tanada S, Boki K, Matsumoto K, 1978. Adsorption properties of methyl sulfide and methyl disulfide on activated carbon, zeolite, and silicate, and their porous structure. *Chemical and Pharmaceutical Bulletin*, 26(5): 1527–1532.

Terazawa K, Mizukami K, Wu B, Takatori T, 1991. Fatality due to inhalation of dimethyl sulfide in a confined space: A case report and animal experiments. *International Journal of Legal Medicine*, 104(3): 141–144.

Wang H T, Zhang Y J, Mu Y J, 2007. Temperature dependence of the absolute rate constant for the reaction of ozone with dimethyl sulfide. *Journal of Environmental Sciences*, 19(6): 641–643.

Warneck P, 2000. Chemistry of the Natural Atmosphere (2nd ed.). Academic Press, San Diego.

Weber R J, McMurry P H, Mauldin R L, Tanner D J, Eisele F L, Clarke A D et al., 1999. New particle formation in the remote troposphere: A comparison of observations at various sites. *Geophysical Research Letters*, 26(3): 307–310.

Yang J T, Shi Y, Chen J, Su Q F, Wang D H, Cao J, 2009. Decomposition of dimethyl sulfide in a wire-cylinder pulse corona reactor. *Journal of Zhejiang University–Science A*, 10(1): 127–132.

Zhang Y F, Allen D G, Liss S N, 2008. Modeling the biofiltration of dimethyl sulfide in the presence of methanol in inorganic biofilters at steady state. *Biotechnology Progress*, 24(4): 845–851.

Zhang Y F, Liss S N, Allen D G, 2007. Effect of methanol on pH and stability of inorganic biofilters treating dimethyl sulfide. *Environmental Science and Technology*, 41(10): 3752–3757.